

Bakery House, 40 High Street, Wimbledon Village, London, SW19 5AU, England Tel: +44 (0)20 8947 7651 Email: phoenics@cham.co.uk Web: www.cham.co.uk

PHOENICS Shines at ZWorld 2025

Wenjun Tan, CAE Product Manager, ZWSOFT

The ZWorld 2025 ZWSOFT Global Ecosystem Conference, themed "Driving Sustainable Industrial Innovation," was successfully held in Guangzhou on August 27th-28th. The conference brought together over 1,000 industry leaders, technical experts, enterprise representatives, and ecosystem partners from more than 30 countries and regions. Through one main summit, 13 industry forums, multiple thematic sessions, and showcases of over 40 industry solutions and collaborative innovation achievements, participants collectively dutlined a new blueprint for the industrial_software_innovation ecosystem, injecting fresh momentum into global industrial sustainability.



During the event, ZWSOFT hosted more than ten industry-specific forums covering machinery & equipment, consumer electronics, automotive parts, mold manufacturing, connectors, architecture, petrochemicals, power, infrastructure, surveying & mapping, simulation applications, AI + Industrial Software, and vocational education. In collaboration with ecosystem partners, ZWSOFT facilitated in-depth discussions and knowledge sharing across multiple dimensions, addressing the practical challenges and efficiency improvement needs of industry users throughout the design, manufacturing, and construction processes. Attendees noted that ZWorld 2025 not only showcased ZWSOFT's latest technological achievements and ecosystem developments but also provided a high-level dialogue platform for the global industrial software industry, fostering cross-disciplinary and cross-regional exchange and cooperation.



ZWCAD + PHOENICS: Reshaping How Cities Breathe with Digital Technology

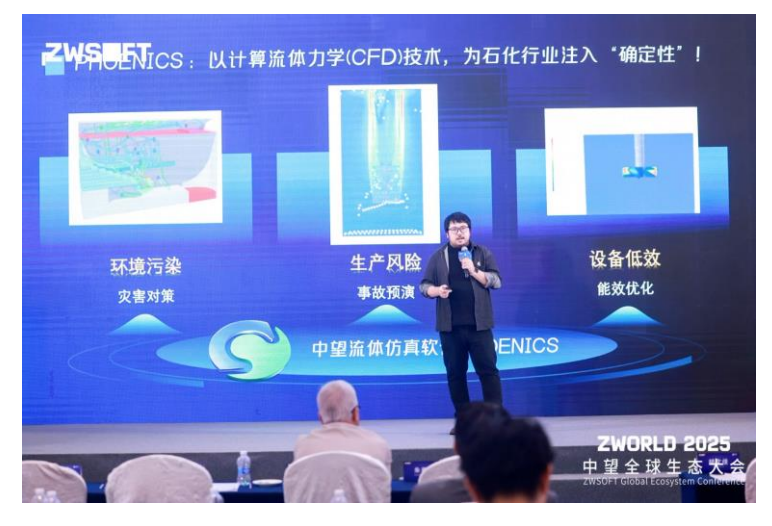
At the main forum, Mr. Lin Qingzhong, Vice President of ZWSOFT, delivered a keynote speech titled "ZWCAD+, Driving Sustainable Industrial Innovation." He presented a real-world customer case involving urban planning in Hong Kong, demonstrating ZWSOFT's integrated "CAD + GIS + CFD" solution.



In this case study, Hong Kong, a typical subtropical high-density city, faces significant urban challenges. To address these, the customer first utilized technologies like oblique photography and laser scanning to acquire realistic 3D geographic data of target areas in Hong Kong, seamlessly importing this massive and complex data into the ZWCAD platform. The 3D city model generated by ZWCAD was then directly imported into ZWSOFT's PHOENICS fluid-simulation software. Based on this model, CFD technology was applied to perform high-precision simulations of the wind and thermal environments in target areas (such as the Tsim Sha Tsui waterfront, Central core district, or new development zones), making the flow of wind and heat visible. These intuitive, quantifiable simulation results, generated by the combined power of ZWCAD and CFD, have become indispensable scientific references for urban planners, architects, and relevant government departments. The combined solution of ZWCAD and PHOENICS has become a essential toolset for numerous architectural engineering consultancies in Hong Kong, driving the city's transition towards becoming a 'climate-adaptive city'.

PHOENICS Empowers the Petrochemical Industry

PHOENICS was featured again at the Petrochemical Industry subforum held in the afternoon. Dr Tan Wenjun, CAE Product Manager at ZWSOFT, presented a report titled "Safety, Environmental Protection, Efficiency: The Application and Value of PHOENICS in the Petrochemical Industry." Through three real customer cases - a CFD analysis of propane dispersion following an LPG storage tank leak, NOx reduction for thermal oxidizer equipment, and the optimised design of jet vacuum pumps - the audience gained insights into how engineers leverage the powerful CFD capabilities of PHOENICS to address a range of engineering challenges in the petrochemical industry from the perspectives of safety, environmental protection, and efficiency.



ZWorld is the annual global ecosystem conference hosted by ZWSOFT, aimed at building a worldwide R&D and design industrial software ecosystem and promoting sustainable industrial innovation through the "CAD+" concept. To learn more about PHOENICS at ZWorld, please visit: lp.zwsoft.com/event/zworld-2025

A Review of Some Recent PHOENICS Publications II

Michael R. Malin, Technical Support Manager, CHAM
Limited

1. Introduction

This article is the second in a series advising readers of some recent PHOENICS-based publications. An earlier Newsletter article [1] summarised some applications published during 2021 to 2023. PHOENICS was the first general-purpose CFD code to appear on the market in 1981 [2], and the last four-and-a-half decades has generated a vast number of publications from both industry and academia. In what follows, a brief summary is provided of recent PHOENICS simulations covering the following areas: hospital-ward ventilation; wind comfort in villages; inertial separation of combustion particles for recycling; and post-operative airflow in the nasal passage.

2. Airflow and Contaminant Dispersion for Hospital-Ward Ventilation Design

In this hospital-ventilation study performed by **UNAM** in **Mexico** [3], **PHOENICS** was used to model airflow and the transport of passive contaminants (pathogen agents) in a multi-bed **intensive care unit** (ICU), which included beds, patients, and HVAC components. The Reynolds-averaged Navier–Stokes (RANS) equations were solved for continuity, momentum, energy and passive contaminants by using the RNG k– ϵ turbulence model; while boundary conditions replicated air-supply diffusers, exhaust outlets, and contaminant sources from patients.

PHOENICS was validated first against two published experimental studies using different ventilation systems in both a climate chamber and a single-patient ICU. Satisfactory agreement between the predictions and measurements was reported in both cases.

For the main ventilation study, transient simulations were performed to cover three air changes and four ventilation systems for an ICU based on the one in Shahid Mustafa Khomeini Hospital, Iran. This unit was the subject of a COVID-9 medical study during the pandemic. The primary objective of these PHOENICS simulations was to aid the development of a ventilation system that prevents the formation of recirculation zones, and achieves the most uniform contaminant concentration possible, thereby minimizing the health problems associated with airborne transmission.

The PHOENICS results showed that airflow patterns had a significant impact on the concentration and removal of contaminants, influenced by geometry and the location of injection ports. In symmetrical injection-port arrangements, contaminant removal proved less efficient than in asymmetrical arrangements. This was due to jet interference and the formation of dead zones by recirculation regions.

3. Wind Comfort Analysis in Traditional Chinese Village Squares

In this study [4], **PHOENICS** was used by **Quanzhou** and **Fujian Universities** to simulate airflow and assess **wind comfort in traditional Chinese-village squares** in Quanzhou City, which is located in the Fujian Province along the southeast coast of China. Through a combination of onsite measurements and PHOENICS simulations, the effects of various layout factors on the winter, wind environment in traditional coastal-village squares were compared and analysed using wind-speed data at a distance of 1.5m above ground, as per China's Green Building Evaluation Standard GB/T 50, 378-2019.

The study used the SketchUp 3D Design Software to create 42 models of traditional village-square spaces, focusing on layout indices rather than architectural details. These models were then imported into **PHOENICS** to perform CFD simulations to assess wind comfort for each village square by considering an array of wind directions in winter. For this purpose, the RANS equations were solved for continuity and momentum by using the RNG k– ϵ turbulence model, applying inlet wind profiles and using nonslip conditions at building and ground surfaces. Overall, PHOENICS produced very good agreement with the measured wind speeds; and these results were used with formulae to analyse how the layout factors of plane permeability, height-to-cross-section ratio, and enclosure rate affected the wind environments of the village squares.

4. Louvre Classifier Design for Unburned Carbon Separation from Biomass Ash

This application from **Hiroshima University**, **Japan** [5] concerns the **inertial separation** of unburned carbon from biomass-combustion ash for recycling purposes. **PHOENICS** was applied to analyse and optimize the performance of a **louvre classifier** designed to separate unburned carbon (UC) from combustion ash. Such inertial-force louvres are used for classifying particles in biomass power plants; and they operate by using a cascade of blades (or louvres) to turn the incoming particle-laden flow into the blade passages, so that the heavier particles resist the directional change and continue onwards into the collection box.

The PHOENICS simulations solved the steady-state RANS equations with the standard k– ϵ turbulence model to predict the airflow inside both a conventional and modified louvre classifier. PARSOL was used to capture the louvre geometry on the background Cartesian mesh, together with nonslip wall conditions and a uniform inlet velocity. The particle motion was simulated using the GENTRA option in PHOENICS, which tracks particles in a Lagrangian frame of reference. The particles were treated as isothermal with sizes ranging from 4 to 150 μ m, whilst exchanging momentum with the flow. The computed trajectories of these particles determined whether they passed through the louvre blades as fine ash, or were collected as coarse ash in the collection box.

PHOENICS was applied to simulate both a conventional and modified louvre classifier. The experimental improvements of the modified louvre classifier were validated by PHOENICS; and key insights were provided into the role of the tilted-sidewall modification, when compared to the performance of a conventional classifier. The simulations showed that the tilted sidewall promoted coarse-ash capture in the collection box, by reducing the upstream flow area and increasing the downward gas velocity in the classification zone, thereby enhancing particle inertia. This matched experimental findings, showing improved separation efficiency and a higher reduction of UC up to 83.8%.

5. Post-Operative Airflow in the Nasal Passage

The **LeFort I (LFI) osteotomy** is a procedure used by maxillofacial surgeons to correct a wide range of dentofacial deformities. However, the procedure may narrow the inferior nasal passage, and this prompted the **Tokyo Medical & Dental University** [6] to use **PHOENICS** in a retrospective study to investigate airflow in the nasal cavities of a sample of patients after one of three different types of LFI surgery, as follows: conventional LFI; LFI with horseshoe osteotomy; and LFI with inferior turbinate partial resection. Coronal computed tomography (CT) images were used to evaluate the degree of stenosis of the inferior nasal passage.

PHOENICS was used to solve the steady RANS continuity and momentum equations with the standard k—ɛ turbulence model, whilst applying steady inspiratory flow at the nostrils and nonslip wall conditions. The nasal airway was modelled using CAD objects extracted from the preoperative and postoperative CT data. The 3D model of the airway (from nostril to larynx) was converted to a smoothed model, but using mesh-morphing software without losing the patient-specific pattern of the airway shape,. The resulting upper-airway CAD file was exported into PHOENICS, and an incompressible air flow, with a specified volumetric flow rate through the nostrils, was applied to simulate inspiration in the upper airway.

Differences between the three patient study groups were evaluated using the nasal flow obtained from the PHOENICS simulations, in the form of flow streamlines, and the pressure and velocity distributions. The findings were that the rate of inferior nasal-passage obstruction was lower in patients who underwent a horseshoe osteotomy or inferior nasal turbinectomy, than in patients who underwent conventional LFI surgery. The addition of a horseshoe osteotomy or inferior nasal turbinate resection was found to be effective in maintaining nasal ventilation.

6. Concluding Remarks

This brief review gives some insight into PHOENICS usage for applications related to pathogen dispersion in hospital wards, wind-comfort assessment in traditional Chinese villages, the inertial separation of unburned-carbon particles in biomass-combustion plants, and the impact of surgery on the airflow in the nasal passage. From time to time, future issues of the Newsletter will provide further reviews of PHOENICS-based publications.

7. References

- 1. M.R.Malin, A Review of Some Recent PHOENICS Publication, PHOENICS Newsletter, Spring Edition, 14-15, (2024)
- 2. D.B.Spalding, A general-purpose computer program for multi-dimensional one- and two-phase flow. Mathematics & Computers in Simulation, 23, 267–276, (1981).
- 3. E.Martinez-Espinosa, W.Vicente, M.Salinas-Vazquez, *Numerical study of the effect of flow patterns on contaminant removal in a hospital ward with symmetrical and asymmetrical inlet port arrangements*, Science of the Total Environment, 979, 179439, (2025).
- 4. Z.Wang, M.Wang, T.Huang, Y.Wang, Y.Zeng, V.Vishnupriya, J.Chen, X.Shen *Evaluation of the influence of traditional village square layout factors on wind comfort*, Building and Environment 267 112160 (2025).
- 5. F.A.Prasetya, T.Fukasawa, T.Ishigami & K.Fukui, Classification performance analysis of a louver classifier with a tilted sidewall and its application to the separation of unburned carbon from biomass combustion ash, Separation and Purification Technology (2025).
- 6. T. Nakamura, N. Tomomatsu, N. Takahara, Y. Kurasawa, Y. Sasaki, T. Yoda, *Morphological changes in the inferior nasal passage associated with superior repositioning of the maxilla with/without horseshoe osteotomy or turbinectomy*. Int. J. Oral Maxillofac. Surg.; 53: 1032–1040, (2024).

Numerical Simulation Study on Liquid Cooling of IGBT for New Energy Vehicles Rainbow Zhu, Senior CFD Engineer, ZWSOFT

1 Introduction

Within the core components of New Energy Vehicles (NEVs), the Insulated Gate Bipolar Transistor (IGBT) plays a pivotal role. It is not only the critical link connecting the power battery and the electric motor, but also a core element determining the vehicle's energy-conversion efficiency and dynamic performance. Particularly in the motor-drive control system, it enables the highly efficient conversion between direct current (DC) and alternating current (AC), allowing the motor to operate stably and providing a powerful source of driving force for the vehicle.

However, during operation, IGBTs generate significant heat due to their inherent power losses. If this heat is not dissipated promptly, and the temperature exceeds the specified safe operating range, the device's performance can degrade significantly. In severe cases, this can lead to permanent damage, posing a substantial threat to the power output and driving safety of the NEV.

In the field of NEV thermal management, liquid-cooling simulation technology has emerged as a core technique to address the thermal challenges of IGBTs. By accurately simulating the flow and heat dissipation processes of the coolant within complex channels, engineers can gain deep insights into the temperature distribution of the IGBT. This enables targeted optimization of the cooling solution, ensuring the IGBT operates reliably within a safe temperature range. Therefore, based on customer requirements, ZWSOFT utilized its fluid simulation software to perform a liquid-cooling simulation analysis of the IGBT, assessing whether its thermal design meets the requirements.

2 The IGBT Liquid-Cooling Simulation Model

2.1 Research Object

The operating ambient temperature for the automotive IGBT module under study is 50° C. The cooling medium is a 50/50 mixture by volume of ethylene glycol and distilled water. The coolant inlet temperature at the cold plate is 60° C, with a flow rate of 15 L/min. The heat dissipation power of a single IGBT is 988 W. The heat dissipation loadings of the other components are annotated on the model in Figure 1. The material for all electronic components is silicon, and the cold plate material is AL6061. The simulation models the IGBT temperature distribution only under liquid-cooling conditions.

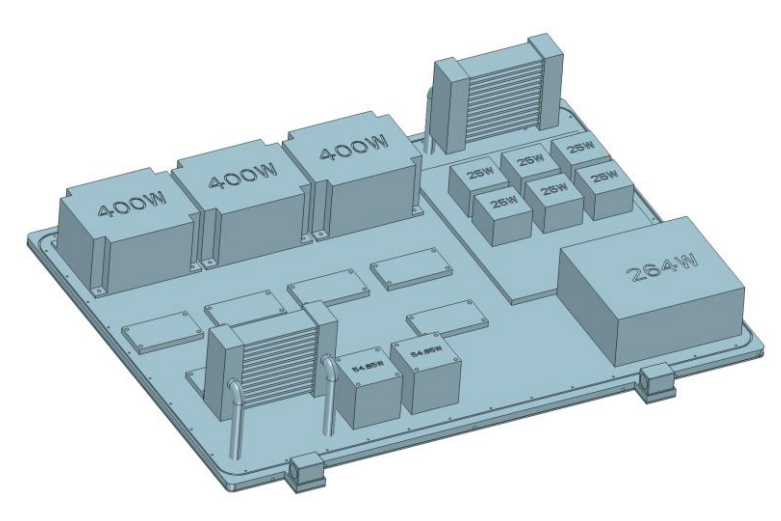


Figure 1. Schematic diagram of the IGBT model.

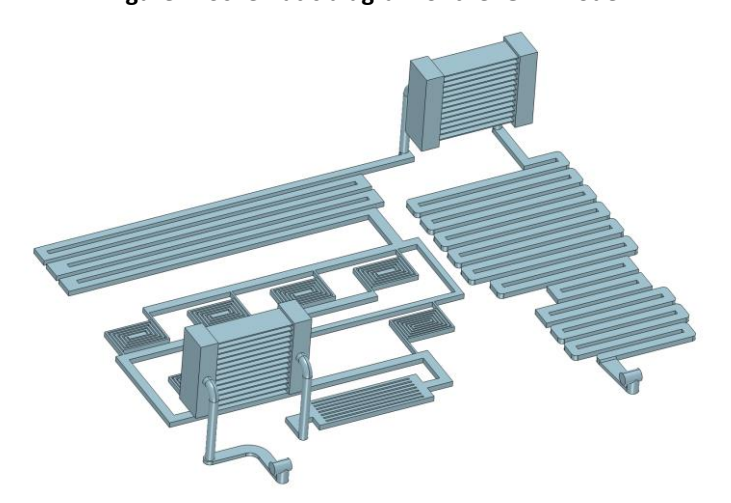


Figure 2. Fluid domain model of the cold plate.

Table 1. Nonlinear thermal conductivity data for Silicon.

Temperature (° C)	Thermal Conductivity [W/(m· K)]
-73	260
26	150
126	99
326	62
526	42

Table 2. AL6061 material properties.

Property	Value
Thermal Conductivity	155 W/(m·K)

Table 3. Ethylene-glycol aqueous solution material properties.

Property	Value
Density	1045 kg/m ³
Kinematic Viscosity	1.1196e-6 m²/s
Specific Heat Capacity	3474 J/(kg·K)
Thermal Conductivity	0.408 W/(m·K)

2.2 Model Assumptions and Numerical Simulation Model

The following assumptions were made for the simulation:

- The fluid flow within the cold plate is assumed to be incompressible.
- The flow is steady-state and turbulent.
- The cold plate outlet pressure is atmospheric.

The standard k- ϵ turbulence model was selected to simulate the complex flow within the cold plate, while balancing computational accuracy and efficiency. Local mesh refinement was applied to small cross-sections within the flow channels to ensure accurate geometric representation, resulting in a final mesh of 5-33 million cells.

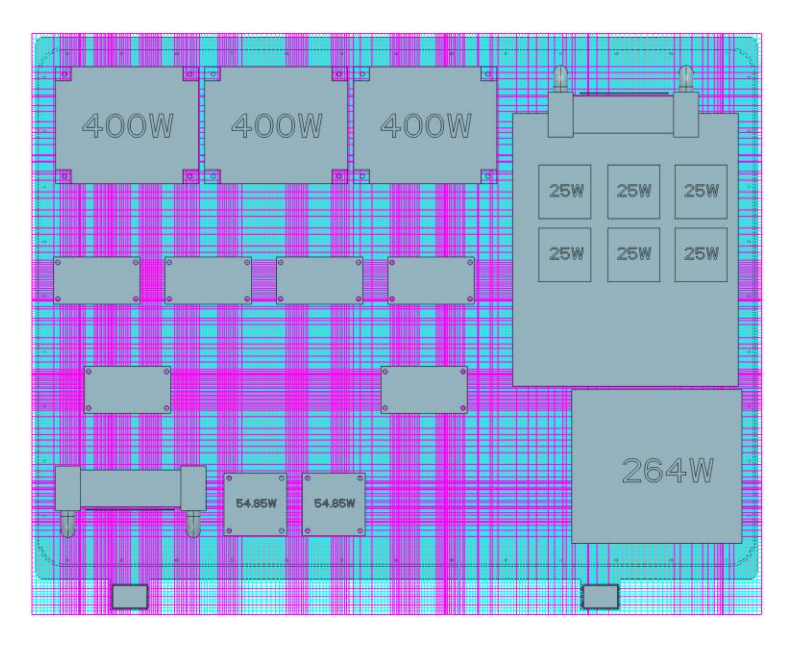


Figure 3. Mesh generation.

3 Results and Discussion

3.1 IGBT Temperature Analysis

The surface temperature contours in Figure 4 show that the maximum temperature is 91.97°C, occurring at the IGBT component nearest the flow-channel outlet. The overall higher temperature of this specific IGBT is attributed to the coolant absorbing heat from upstream IGBTs, causing its temperature to rise gradually. The maximum IGBT temperature is below 130°C, and the temperatures of other electronic components are all below 80°C, indicating that the IGBT module meets the thermal design requirements.

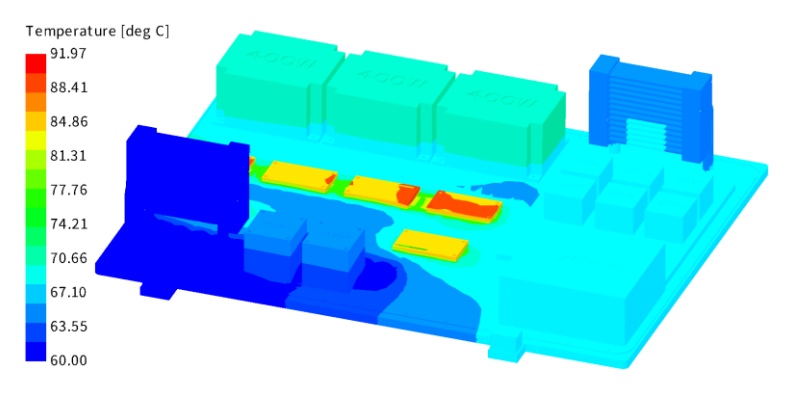


Figure 4. Surface temperature contour plot of the components.

3.2 Internal Flow Analysis of the Cold Plate

A cross-section was created through the middle of the cold-plate's cooling channels. Temperature and velocity contour plots were generated for this section, as shown in Figures 5 and 6, respectively. The results indicate that the high-temperature regions within the cold plate are primarily distributed beneath the IGBTs. The maximum temperature of the coolant directly below the IGBTs is approximately 83°C. The temperature in the left-hand flow channel is relatively lower, because the heat dissipation from components in this area is comparatively lower, and the contact area with the cold plate is larger. The flow velocity in most areas of the cold plate is about 2 m/s, with a maximum velocity of 3.79 m/s. Within the narrow cooling channels

in the IGBT region, the flow velocity is approximately 1.5 m/s. This flow velocity is sufficient to rapidly remove heat from the IGBT module.

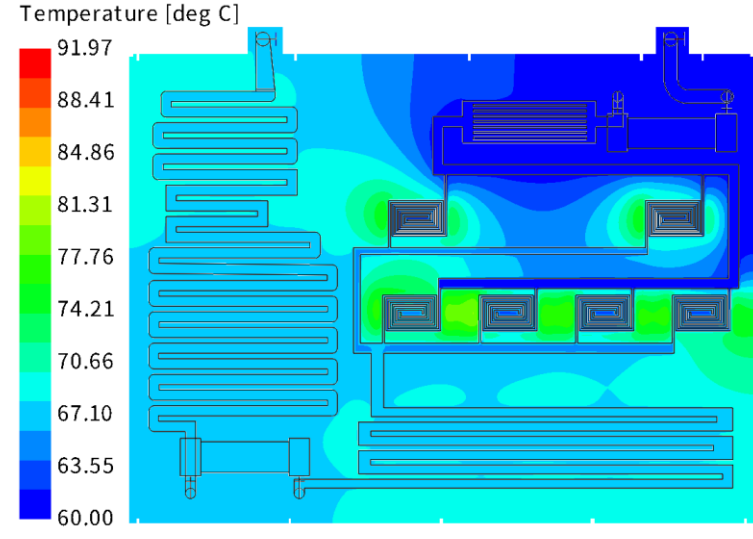


Figure 5. Temperature contour plot of the cold-plate cross-section.

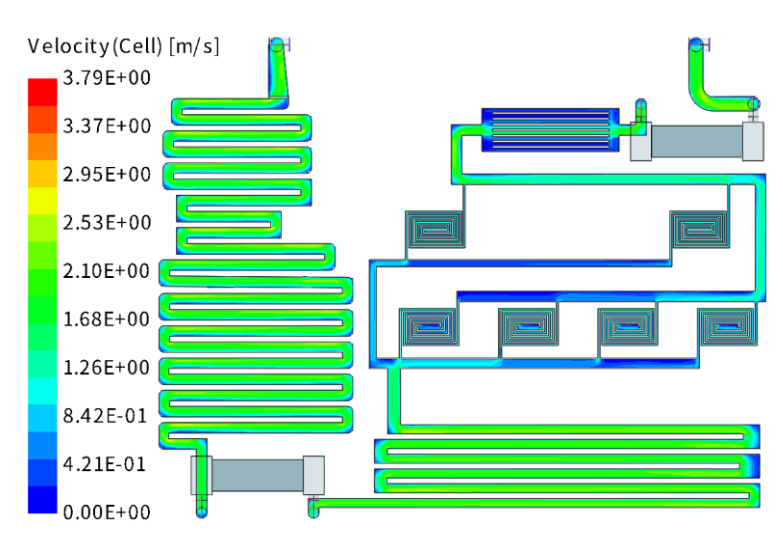


Figure 6. Velocity contour plot of the cold-plate cross-section.

3.3 Cold Plate Inlet/Outlet Analysis

Temperature and pressure contour plots were generated for the coldplate inlet and outlet, as shown in Figures 7 and 8, and the temperature and pressure at the centre points were probed. The results show an inlet temperature of 60.0°C and an outlet temperature of 68.4°C, resulting in a coolant temperature rise of 8.4°C across the flow channels. The inlet pressure is 155,209 Pa, and the outlet pressure is 0 Pa (atmospheric), resulting in a total pressure drop of 155.2 kPa across the cold plate.

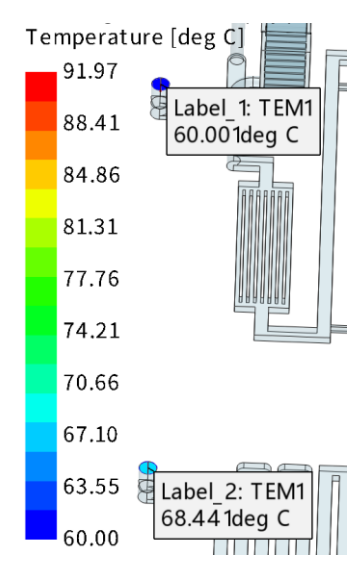


Figure 7. Inlet/Outlet temperature contour plot and result probing.

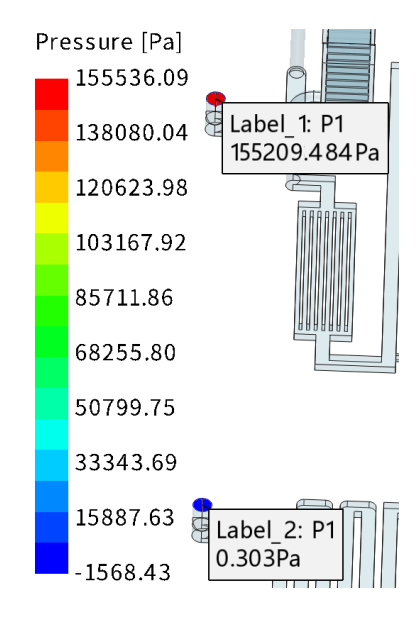


Figure 8. Inlet/Outlet pressure contour plot and result probing.

4 Conclusion

This study established a numerical model for the liquid cooling of an IGBT using ZWSOFT's fluid simulation software, successfully performing the liquid-cooling simulation analysis. The main conclusions are as follows:

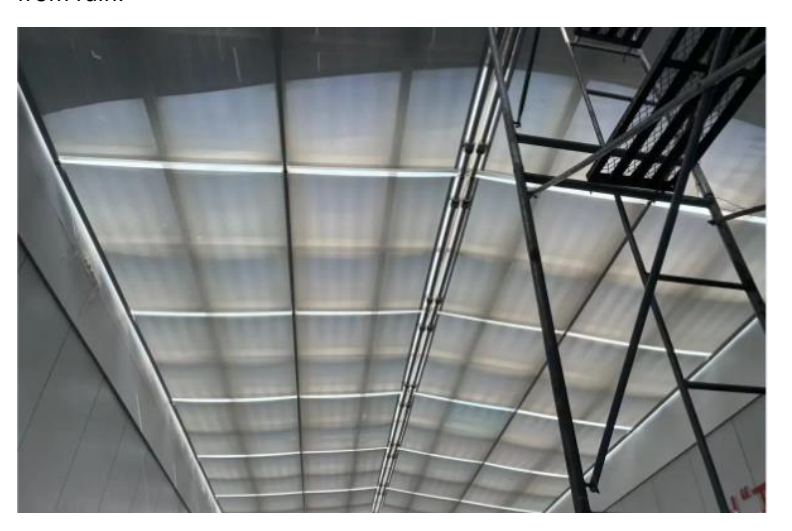
- The IGBT exhibits the highest temperature in the entire model, at 91.97° C. As this maximum temperature is below 130° C, the design meets the thermal requirements.
- The maximum temperature of the coolant is approximately 83°
 C, with the high-temperature regions primarily located in the narrow cooling channels directly beneath the IGBTs.
- 3. The cold plate inlet temperature is 60.0° C, and the outlet temperature is 68.4° C, resulting in a coolant temperature rise of 8.4° C through the channels.
- 4. The cold-plate inlet pressure is 155,209 Pa, and the outlet pressure is 0 Pa, resulting in a pressure drop of 155.2 kPa across the channels.

Wind Resistance Assessment of a Retractable Shading Canopy in a Residential Community

Wenjun Tan, CAE Product Manager, ZWSOFT & David Glynn, Consultant, CHAM

1. Problem Background

A retractable shading canopy is a flexible or semi-rigid shading structure that can be deployed or retracted via an electric control system. It is widely used in outdoor spaces such as commercial streets, residential communities, and stadiums to provide shading and shelter from rain.



Its main benefits include:

- Microclimate Regulation: Effectively blocks sunlight, reduces surface temperature, and improves comfort for outdoor activities.
- Enhanced Spatial Quality: Integrates with architectural aesthetics to create visual focal points and strengthen place identity.
- Energy Saving & Environmental Protection: Reduces air conditioning energy consumption and promotes natural ventilation and lighting.

A Shanghai-based architectural design institute was commissioned by the client to be responsible for the overall design of the landscaping and recreational environment for a residential community. A retractable shading canopy, located in the central activity area of the community, is a core feature of the project. To ensure the structural safety and operational reliability of the canopy under strong wind conditions, the design institute needed to perform a numerical-simulation analysis of its wind resistance, and subsequently select the most suitable type of canopy for deployment

2. CFD Modelling and Technical Challenges

(1) Canopy Geometry Processing

The initial canopy geometry was provided in Rhino format (.3dm), and was then imported into ZW3D 2026 for conversion into z3prt format. The following was used to prepare the model for subsequent CFD analysis:

- Geometry Integrity Check: Ensured surface closure and absence of gaps.
- Smoothing Treatment: Adapted the geometry for PHOENICS's Cartesian-grid system to improve computational stability.

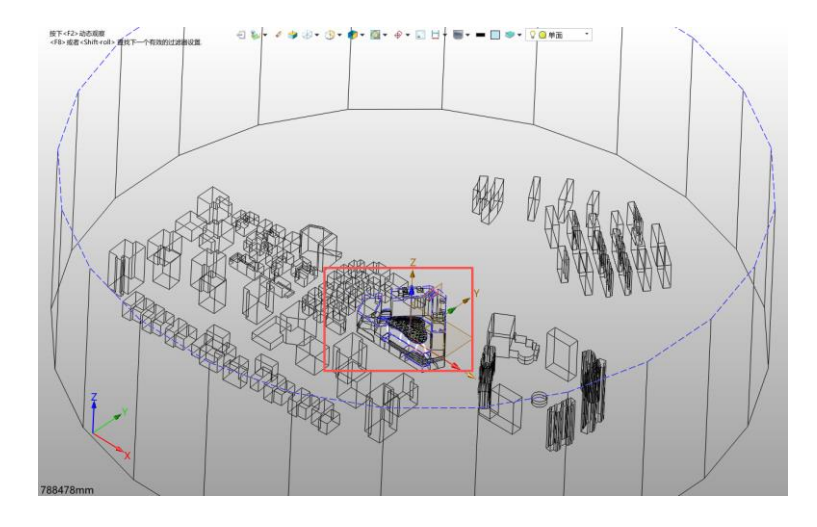


Fig.1 Urban area model; the red box indicates the target residential community.

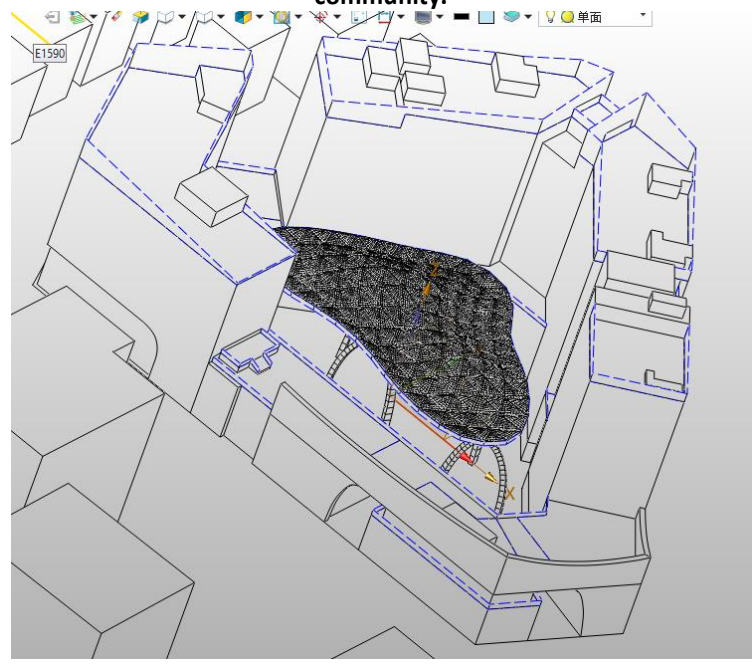
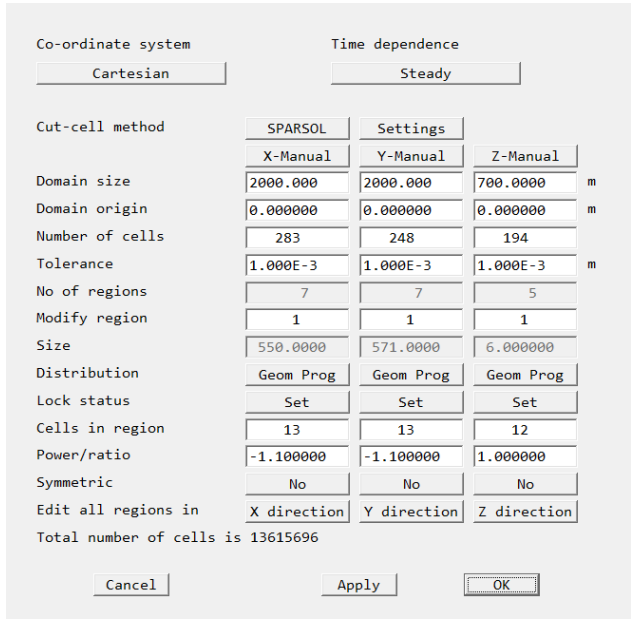


Fig.2 The retractable shading canopy in the community centre; smoothing its surface was one of the technical challenges of this project (ZW3D handled this task easily).

(2) Meshing

Meshing was performed using PHOENICS with the following parameters:

- Grid Type: Structured Cartesian grid.
- **Grid Count**: 283 × 248 × 194, totaling approximately 13.6 million cells.
- **Local Refinement**: A high grid density was applied around the canopy region to capture detailed flow features.
- Advantages: Rapid grid generation, high computational efficiency, suitable for far-field treatment with coarser grids.



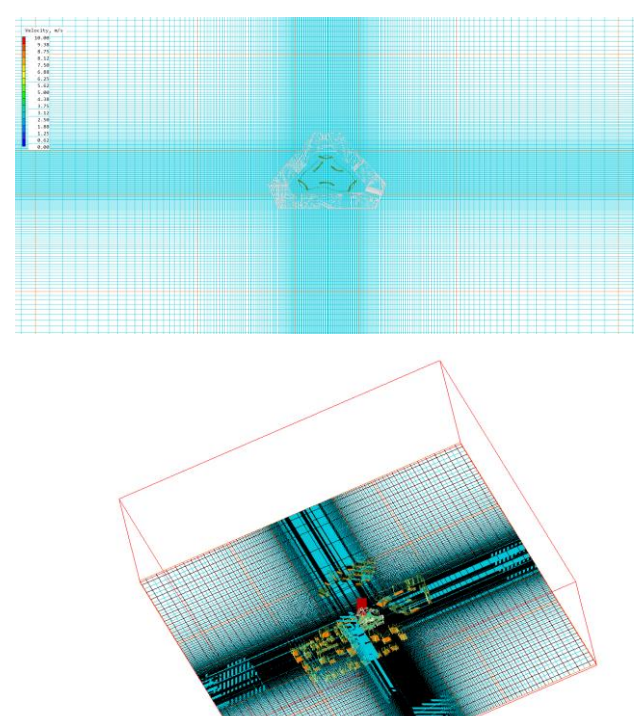


Fig.3 The mesh; anisotropic refinement was applied at the target community area.

(3) Boundary Conditions Setup

• **Wind Velocity Profile**: For the atmospheric boundary layer, a power-law velocity distribution was employed:

$$v(z) = v_0 (\frac{z}{z_0})^{\alpha}$$

where the basic wind pressure was 0.55 kPa, corresponding to a wind speed of 15.7 m/s at the reference height. The ground roughness category was Class B, with α taken as 0.15.

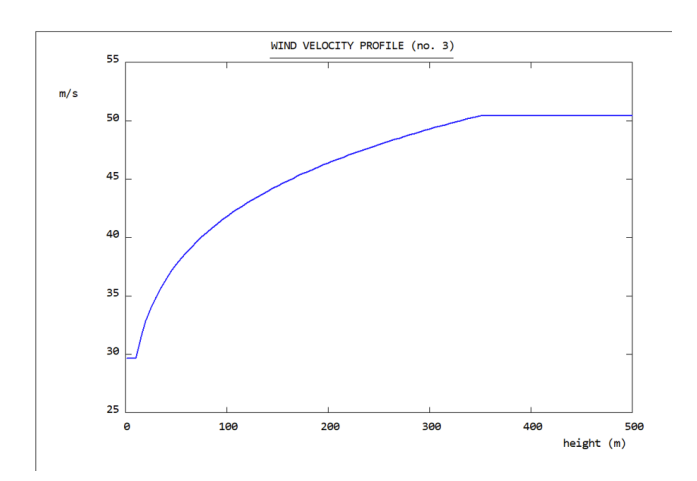
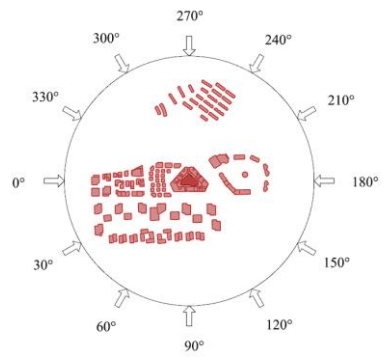


Fig.4 Wind speeds at various heights were calculated and tabulated at 1-metre intervals, then imported into a custom wind profile.

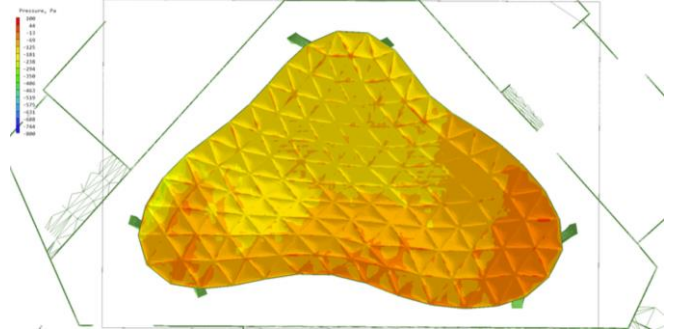
- Turbulence Model: The standard k-ɛ turbulence model was used, with the turbulence intensity of the wind field set at the domain boundaries in accordance with the Japanese Architectural Load Standard (2004).
- Wind Direction Simulation: The project simulated multiple wind-direction angles including 0°, 90°, 120°, 150°, 180°, 210°, 240°, and 270°. Due to space limitations, this article only presents the wind-load distribution results for the 0° wind direction (due east).



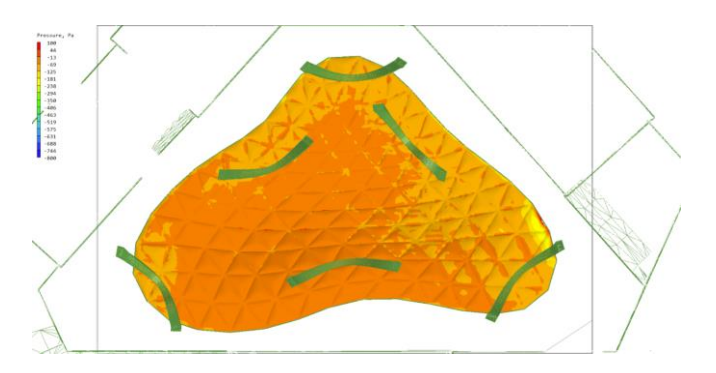
3. Result Analysis

(1) Pressure Distribution

 Upper Surface: Overall, the wind pressure distribution was relatively uniform, showing a general downward-pressure trend.
 The maximum wind pressure occurred in the windward region.



 Lower Surface: The wind pressure distribution was complex, with significant negative pressure zones. Local low pressure occurred particularly in the south eastern corner area, potentially causing uplift forces.

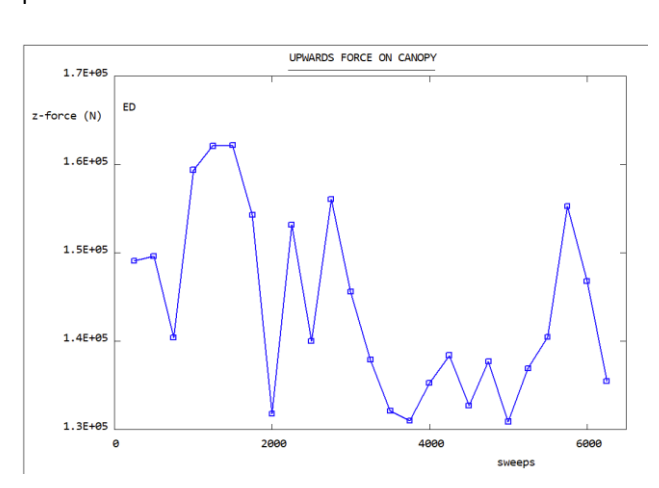


• Wind Speed Distribution: Wind speeds at 1.5m height within the community were generally low, meeting pedestrian comfort requirements.

(2) Extraction of Pressure Difference Between Upper and Lower Surfaces

Pressure and velocity data at key points (e.g., coordinates (95,98,29)) were extracted via PHOENICS to calculate the pressure difference between the upper and lower surfaces, and then used to evaluate the net wind load on the canopy. The results indicated that:

- The canopy experiences positive pressure under most winddirection angles.
- Negative pressure exists in local areas, requiring attention to antiuplift measures and local reinforcement.



4. Suggestions for Improved Simulations:

9

- Suggestion 1: The wind-speed boundary condition shown in Figure 4 is overly simplified because uniformity is assumed below 10 m, and above 350 m. In particular, below 10m, boundary-layer theory can be used to generate a more realistic velocity profile which accounts for ground friction.
- Suggestion 2: Employ transient calculations so as to resolve any unsteady features such as vortex shedding. This can be expected to yield monotonic convergence behaviour at each time step, albeit at greater computational expense. If the client does not require this more accurate result, then steady-state calculations are still sufficient to address the key concerns

3. Suggestion 3: Reduce the size of the global computational domain and allocate the saved computational resources to focus on the target community area. We estimate that halving the length of the domain space would not significantly affect the current results. For the top boundary, rather than use the default zero-flux condition, the domain height can be reduced and PHOENICS's 'open sky' function applied together with a fixed-pressure condition to account for turbulent transport on the assumption of a uniform shear stress.

4. Conclusions

A wind-load simulation analysis of the retractable shading canopy was carried out using the PHOENICS software, and this led to the following conclusions:

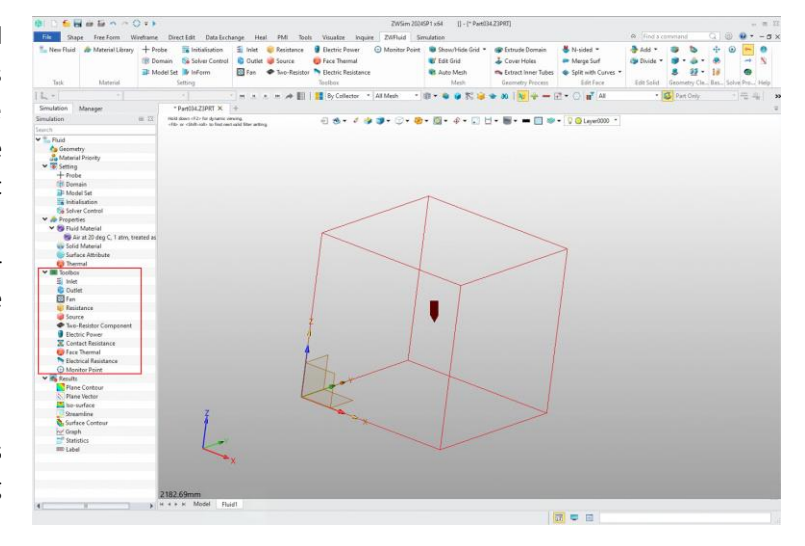
- Clear Wind Pressure Distribution: The upper surface of the canopy is predominantly under positive pressure, while the lower surface exhibits complex negative pressure zones that must be considered in the structural design.
- 2. **Good Pedestrian Wind Comfort**: Wind speeds are significantly attenuated inside the community, meeting comfort requirements for pedestrian activities.
- Structural Type Recommendation: It is recommended to select a canopy type with sufficient rigidity and wind uplift resistance, with local reinforcement applied in low-pressure areas such as the south eastern corner.

This simulation analysis provides a reliable basis for the structural selection and optimization of the canopy, demonstrating the important role of CFD technology in modern architectural wind engineering.

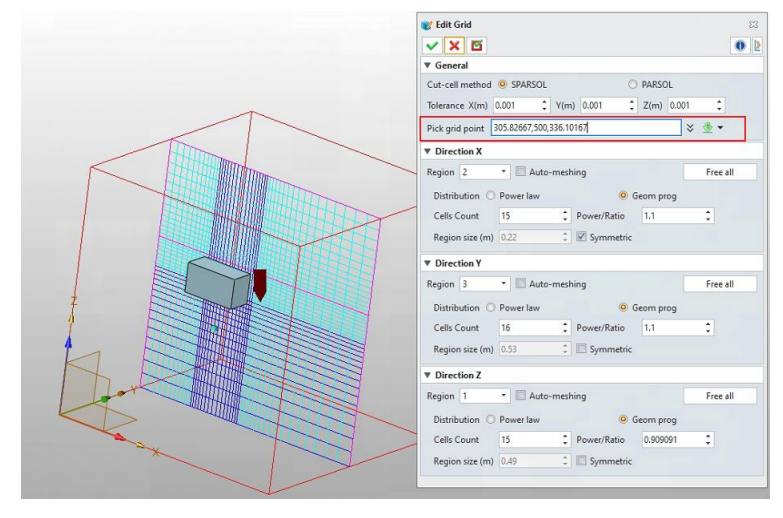
From PHOENICS to ZW3D Flow: A brief introduction to recent R&D progress

Isaac Wang, Senior CFD Engineer, ZWSOFT

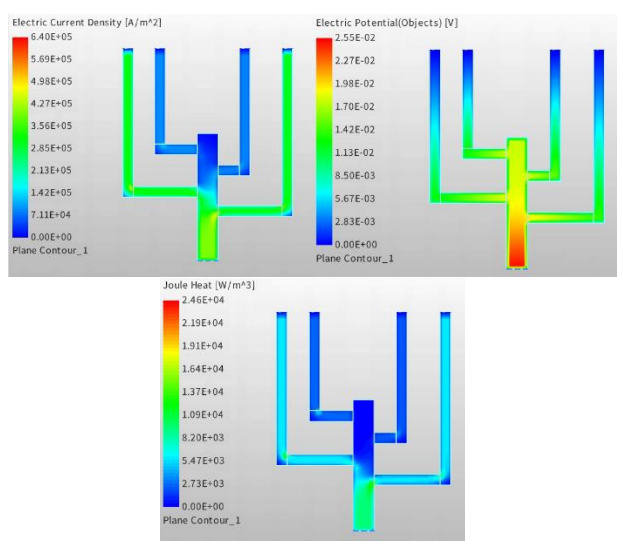
Traditional CFD workflows often require switching between multiple software platforms for modeling, meshing, solving, and postprocessing, resulting in complex processes and inefficiency. The deep integration of PHOENICS's mature solver capabilities with the powerful modeling, pre-processing, and post-processing functionalities of the ZW3D platform enables users to complete geometry modeling, fluid simulation, and result analysis seamlessly within the ZW3D environment, significantly reducing learning curve and usability barriers. Furthermore, many industry users (e.g., in general machinery and equipment) require a reliable yet easy-to-use fluid simulation tool. Leveraging the algorithmic advantages of PHOENICS, ZW3D Flow can not only handle complex flow and heattransfer problems but also provide engineers and designers with trustworthy simulation results to support structural optimization and performance enhancement. This integrated solution is the fundamental driver behind our functional migration initiative.



The pre-processor of the ZW3D Flow plugin possesses robust geometry modeling and simplification capabilities. For simulation, it supports both steady-state and transient simulations of fluid flow, handling various flow characteristics including compressible and incompressible flows for gases and liquids. It analyzes thermal convection, conduction, and radiation, supporting heat exchange analysis between fluids and solids. The setup of various boundary conditions such as inlet, outlet, wall, and symmetry plane is supported, offering flexibility to adapt to different simulation requirements. In terms of meshing, a pointselection mesh tool is provided to facilitate rapid mesh editing for users. After enabling mesh display, clicking on a specific mesh quickly locates the corresponding region for mesh-related edits, significantly enhancing mesh- editing efficiency. The ZW3D Flow SP version, scheduled for release by the end of this year, will continuously improve functionalities. New additions to the Toolbox include planar heat sources, planar thermal resistance, planar electrical resistance, and Joule heating, further enhancing its capabilities for applications in general machinery and electronics cooling.



Simultaneously, for post-processing, simulation results can be analyzed using methods such as contour plots, vector plots, and streamlines. Compared to PHOENICS's post-processing, the display efficiency and methods have been optimized, making result visualization more efficient and intuitive. Added functionalities like data statistics and animation display assist engineers in quickly analyzing results after simulation completion and proposing product optimization plans. The figures below show a Joule-heating analysis for a copper busbar, in terms of contour plots of the current density, voltage, and Joule heating, respectively.



In summary, the ZW3D Flow plugin has already made significant progress in terms of functional breadth and industry applicability, demonstrating strong capabilities for solving typical problems in industries, such as general machinery and electronic equipment. Future versions will focus on continuous optimization in the following key areas:

(a) Meshing Technology, by introducing more advanced mesh generation and adaptation schemes (e.g., the inclusion of unstructured meshing technology through Unstructured PHOENICS (USP)); (b) Solver Performance, further enhancing solution accuracy and computational efficiency, aiming for the ZW3D Flow plugin to be not only simple to use, but also fast and accurate in computation; (c) User Experience, maintaining operational simplicity, while making computations faster and more accurate.

ZW3D Flow will continue to provide engineers and designers with efficient and accurate simulation tools, helping users rapidly resolve engineering design challenges, create greater value, and enhance enterprise competitiveness.

Photo Gallery: ZWSOFT Headquarters Relocation Celebration

On 1 August 2025, ZWSOFT officially moved into its new headquarters building – ZWSOFT Tower. The images below capture scenes from the relocation ceremony held on that day.



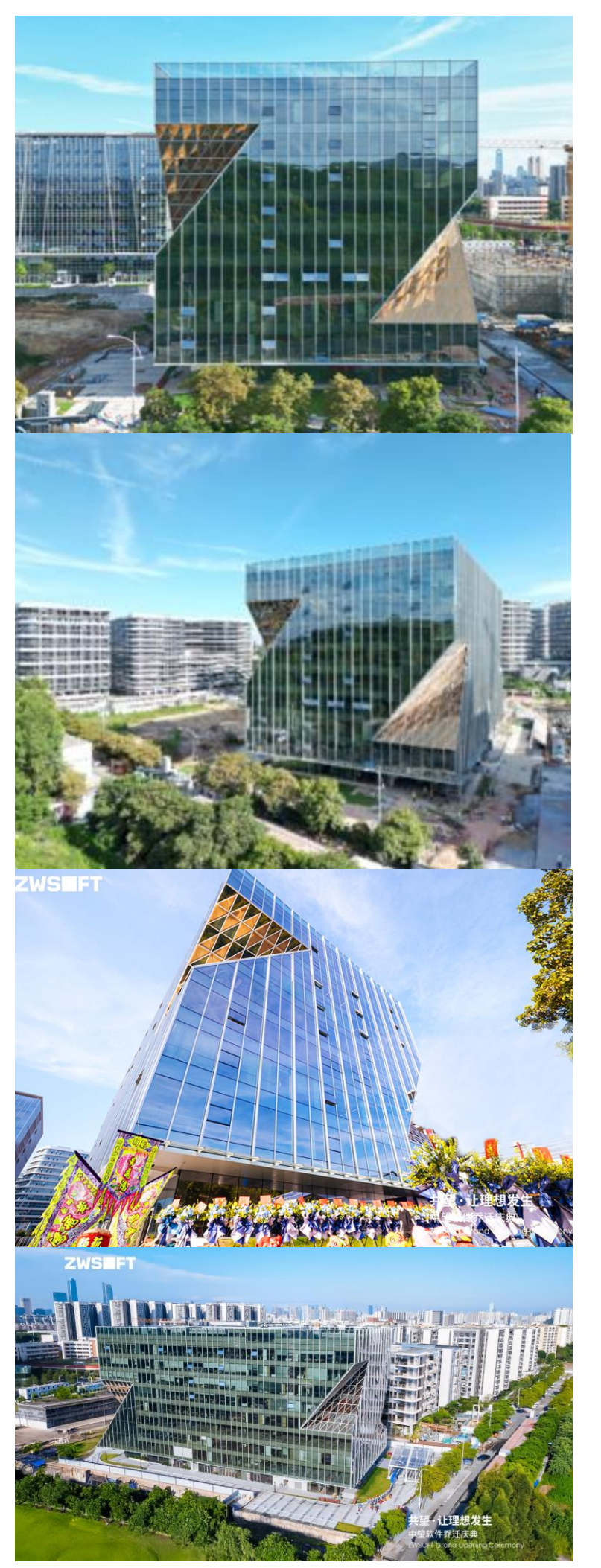


A traditional Lion Dance performance, rich in Chinese cultural significance. In China, relocating to a new office is a momentous and joyous occasion, often celebrated with Lion Dances to express positive aspirations for the future.



Construction of ZWSOFT Tower began in October 2021. After four years, the project successfully passed final inspection and acceptance. Located in Guangzhou's core business district, the building's distinctive overall silhouette is inspired by the letter 'Z', the initial of ZWSOFT. With 11 floors, it has become a notable local landmark.









Bright, spacious, open-plan work areas capable of accommodating over 1,000 employees.



Numerous breakout areas provide employees with a relaxed and comfortable working environment.







Facilities including a gym, billiards room, and library are available for employees to use free of charge. These amenities promote work-life balance, allowing staff to relax and recharge, thereby enabling them to focus more effectively on their work



CHAM would like to welcome our newest member of staff



Dr David Jones

Dr David Jones joined us recently from Swansea University as a CFD Development Engineer, having successfully completed his PhD in CFD from Swansea University with a Thesis entitled "A Second-Order Accurate Mach-Uniform Scheme for the Unsteady Compressible Navier-Stokes Equations on Orthogonal Unstructured Grids."

Contact Us:

CHAM's highly skilled, and helpful, technical team can assist in solving your CFD problems via proven, cost-effective, and reliable, CFD software solutions, training, technical support and consulting services. If YOU have a CFD problem why not get in touch to see how WE can help with the solutions?

See us on social media sites shown below:









